RSC Advances

ROYAL SOCIETY OF CHEMISTRY

www.rsc.org/advances

Synthesis, characterization and theoretical calculations of model compounds of silanols catalyzed by TEMPO to elucidate the presence of Si-O-Si and Si-O-N bonds.

Judith Percino[1*], José A. Pacheco[1], Guillermo Soriano-Moro[1], Margarita Cerón[1], M. Eugenia Castro[1], Víctor M. Chapela[1], José Bonilla-Cruz[2], Tania E. Lara-Ceniceros[2], Mildred Flores-Guerrero[2] and Enrique Saldivar-Guerra[3].

[1]*Lab. de Polímeros, Centro de Química, Instituto de Ciencias, Benemérita Universidad Autónoma de Puebla, Complejo de Ciencias, ICUAP, Edif. 103H, 22 Sur y San Claudio, C.P. 72570 Puebla, Puebla, México.*

[2]*Cento de Investigación en Materiales Avanzados S.C. (CIMAV-Unidad Monterrey), Alianza Norte 202, Autopista Monterrey-Aeropuerto Km 10, PIIT, C.P. 66600 Apodaca, Nuevo León, México.*

[3]*Centro de Investigación en Química Aplicada, Blvd. Enrique Reyna No. 140, Col. San José de los Cerritos, C.P. 25294 Saltillo, Coahuila, México.*

Corresponding author:
M. Judith Percino,
Centro de Química, Instituto de Ciencias,
Benemérita Universidad Autónoma de Puebla,
Complejo de Ciencias, ICUAP, Edif. 103H,
22 Sur y San Claudio, C.P. 72570,
Tel. +52-222-2295500 x 7285
judith.percino@correo.buap.mx

1

Abstract

We report the results from the reactions of the 1-phenylethanol, 2-methylpropanol, trimethylsilanol and triphenylsilanol with TEMPO, OH-TEMPO and Br-TEMPO salt at different reaction conditions to obtain model functionalized compounds. With 1-phenylethanol, the ketone compound was obtained as expected, but using the triphenylsilanol the corresponding hexaphenyldisiloxane [di(triphenylsilane)ether] was obtained in crystal form, as well as, the silaneoxiamine (Si-O-N). The hexaphenyldisiloxane crystal belonged to the triclinic crystal system with a space group *P-1, a* = 8.5829(4) Å, *b* = 9.4856(4) Å, *c* = 10.9694(5) Å, α= 95.951(4)°, β= 90.059(3)°, γ=113.352(4)°, the asymmetric unit comprised of *Z*=1. The results showed that the synthetic method to obtain silane ether is simple and can be completed in one step, as well as independently of the type of TEMPO and base used. Also, under the same reactions conditions, we prepared the corresponding TEMPO-containing silanes as triphenylsilaneoxiamine and observed formation of Si-oxide chains through an *in situ* polycondensation reaction. The resulting compounds were characterized by FT-IR spectroscopy, mass spectrometry (EI), and ^{1}H-NMR. A best assignment for infrared spectroscopy characterization and the structural parameters by vibrational frequencies were determined by DFT calculations.

Keywords

Introduction

Symmetrical disiloxanes are an important class of compounds in silicon chemistry.[1] Some of the symmetrical disiloxanes are known to have important applications as liquid crystals,[2-7] and pharmacologically active compounds.[8-9] Recently, some of these compounds have drawn attention as useful intermediates in organic synthesis. Napier et al.[10] and Sore et al.[11] have shown novel applications of aryl disiloxanes and vinyl disiloxanes, respectively, as efficient coupling partners in Hiyama cross-coupling reactions. The general methods available in the literature for the preparation of symmetrical disiloxanes are intermolecular condensation of silanols,[12,13] and reaction of polysiloxanes with Grignard reagents.[14,15]

On the other hand, it is well know that silica plays an important role in nature, science, and technological applications.[16-18] The chemical properties of the silica surface are mainly determined by several silanol and siloxane groups that are present on both the external and internal surfaces. Silanol groups (SiOH) can be easily functionalized by different chemical procedures,[16-23] and the importance of functionalized silica materials is due to its applications in chromatography among others.[24-27] The chemical functionalization of silicon dioxide (SiO_2) surfaces with silane molecules is an important technique for a variety of device,[28-31] and sensor applications.[32-33] However, the quality control of self-assembled monolayers (SAMs) is difficult to achieve because of the lack of a method to directly measure the formation of new interfacial Si-O bonds. Tian et al. reported a direct characterization of the interfacial Si-O bond formation,[34] which extended our understanding of the surface reaction mechanisms and improved the quality of the SAM. Infrared spectroscopy has also been used in the silica powder surface silanization studies for monitoring Si-O-Si bond formation.[35] By monitoring the Si-O-Si region of the IR spectrum,

it is possible to distinguish between an organosilane that is covalently bound through Si-O-Si surface bonds and an organosilane polymer deposited on the surface.

Moreover, various functionalized alkoxyamines have been designed and synthesized as initiators for living free radical polymerization, leading to well-defined macromolecular architectures, such as block, graft, and star polymers.[36-41] Since Hawker et al. reported the synthesis of 2,2,6,6-tetramethyl-l-(1-phenylethoxy)-piperidine from the reaction of 2,2,6,6-tetramethylpiperidine-1-oxyl (TEMPO) and an excess amount of styrene in the presence of benzoyl peroxide,[38] a few synthetic methods for alkoxyamines have been reported. For example, ethylbenzene derivatives were reacted with the *tert*-butoxyl radical (*tert*-BuO) and then coupled with the nitroxyl radical.[39,40]

In addition, the polymer-coated nanoparticles are of great interest because of their applications, one of the most effective methods to polymer-coated nanoparticles is surface functionalization by grafting of polymer. The surface properties can be widely varied by choosing diverse functional monomers.[41-49] Thus, different nanoparticles, such as silica, carbon, could be functionalized with well defined polymers of the desired grafting density, to interact wih iron, gold, silver particles. To date, surface initiated graft polymerization can be used to control the molecular weight of the graft chains on nanoparticles by using of living radical polymerization technique, i.e. atom transfer radical polymerization (ATRP), and reversible addition-fragmentation transfer (RAFT). For example, Matyjaszewski et al. has been synthetized organic/inorganic hybrid nanoparticles by ATRP using silica functionalized with ATRP initiator groups.[50] Benicewicz et al. has been grafted silica nanoparticles by RAFT in order to obtain dye labeled polymers[51] or stabilize magnetic nanoparticles with biomedical applications.[52] Recently, Bonilla et al. had proposed the functionalization of particles of silica using a TEMPO-bromide salt (Br-TEMPO) in order

to grow styrene-maleic anhydride copolymers from the functionalized silica surface.[53] These investigators proposed that the hydroxyl groups on the silica surface are potential sites for attack by Br-TEMPO salt, according to Scheme 1. By use of undirected experiments by GPC and DSC, these studies showed that the particles were functionalized and verified the growth of the polymers chains.[41,53] However, there was no direct observation of the formation of the N-O-O-Si moiety in the silica.
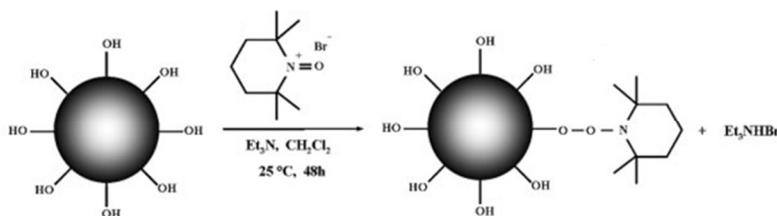
Scheme 1. Procedure for preparing PSMA-NMRP particles, as proposed by Bonilla *et al.* [53]

Therefore, it is important to understand the surface reaction mechanisms. Present methodology cannot determine whether the newly formed organosilanes are parts of the silica network or are attached through just one bond. The difficulty in discovering the nature of the interfacial Si-O bonds arises from the complexity of distinguishing if the bond is present as Si-O-Si, Si-O-N, or as the proposed Si-O-O-N bond formation in the model compounds. In the present work we report model compounds from reactions of silanols catalyzed by TEMPO to determine the type of bond present (e.g., N-O-Si or Si-O-Si) after surface-grafting of nanomaterials via the surface-initiated nitroxide-mediated radical polymerization (Si-NMRP) approach.

Experimental

Materials and Instrumentation

1-Phenylethanol, 2-methylpropan-2-ol, trimethylsilanol, triphenylsilanol, TEMPO, OH-TEMPO, oxo-TEMPO and NH_2-TEMPO were acquired from Aldrich Chemical Co. Melting points were measured with an SEV (0-300 °C) apparatus and were reported as uncorrected values. IR spectra of the products were recorded on a Vertex (model 70, Bruker Optics, Germany) 750 FT-IR spectrophotometer by attenuated total reflectance (ATR). ^{1}H NMR and ^{13}C NMR spectra were obtained in $CDCl_3$ and DMSO-d_6 on a Bruker 500 MHz NMR spectrometer (Varian NMR, Walnut Creek, CA). The electron ionization (EI) spectra were acquired on a Jeol MStation 700-D mass spectrometer (Jeol USA, Peabody, MA).

Differential scanning calorimetry (DSC) curves were acquired with a TA Instruments DSC Q200. Typically, 1–2 mg of the sample was added to an aluminum pan (Tzero®) and heated at 10 °C min^{-1} in the range of -10 °C to 400 °C. The sample was cooled at the same rate of 10 °C min^{-1} up to 25°C. Scanning electron microscopy (SEM) of Field Emission Model 200 Nova NanoSEM (FEI Company) was utilized at 15kV to investigate the morphology of new compouds.

The synthesis of 2,2,6,6-tetramethyl-1-oxopiperidinebromide salt (Br-TEMPO) was carried out according to a literature procedure (Scheme 2).[54] Bromine (1.64 mL, 32 mmol) was carefully measured using a glass syringe and was added slowly to a solution of TEMPO (5 g, 32 mmol in 100 mL of CCl_4 anhydrous). A brown solid (Br-TEMPO) was formed instantaneously and was purified by washing with CCl_4. The Br-TEMPO salt was dried under vacuum at room temperature overnight (yield 92%). ^{1}H NMR (400 MHz, CDCl_3): 2.32–2.74 ppm (m, 6H, CH_2), 1.71–1.99 ppm (s, 12H, CH_3).
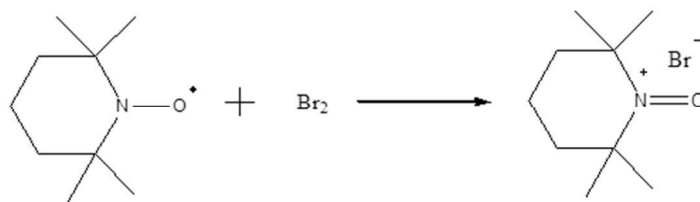
Scheme 2. Synthesis of the oxoammonium salt (Br-TEMPO).

Oxidation of methylbenzylalcohol to acetophenone

The Br-TEMPO salt is well known to be a good oxidant. We used Br-TEMPO as an oxidizing agent in the following manner (Scheme 3): under magnetic stirring, 1-phenylethanol (0.15 g, 1.27 mmol) was added dropwise to Br-TEMPO (0.3 g, 1.27 mmol) dissolved in 3.5 mL of dichloromethane simultaneously with a 37% NaOH solution. The reaction mixture changed from brown to orange over approximately 5 min. At the end of reaction, the solid phase was isolated by filtration and the liquid phase solvent was evaporated under vacuum. The liquid concentrate was analyzed by IR and ^{1}H-NMR.
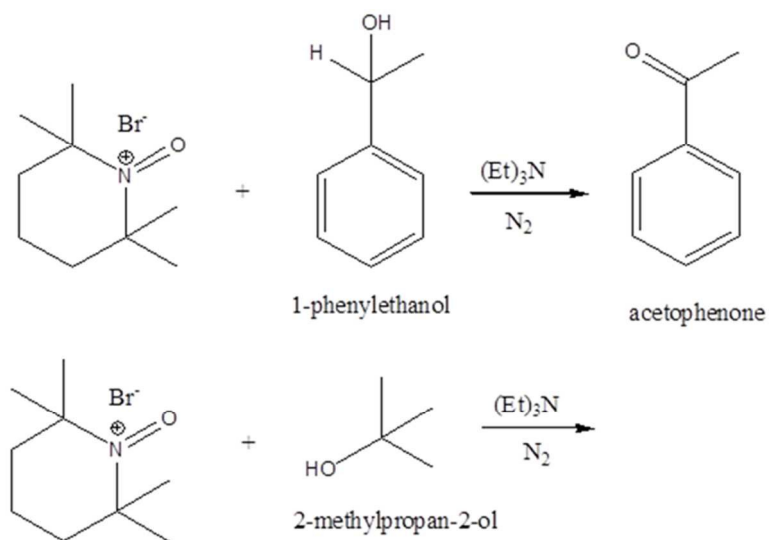
Scheme 3. Synthesis of acetophenone (top) and the reaction of 2-methylpropan-2-ol

(bottom) using Br-TEMPO

7

Reactions of 2-methylpropan-2-ol, trimethylsilanol, triphenylsilanol at different reaction conditions

The reaction conditions of temperature, time, and amount of Br-TEMPO were examined to optimize the functionalization of the nanoparticles through the formation of the peroxide bond as: –N-O-O-Si- (Table 1).[53] Additional reaction conditions were selected because preliminary experiments demonstrated that the reaction did not require the use of the bromine salt of TEMPO. Hence, we developed the following general reaction procedure: a mixture of triphenylsilanol (1.08 mmol, 0.3 g) with TEMPO at molar ratio (1:1) was maintained at reflux and stirred at 67 °C. Triphenylsilanol (1.08 mmol, 0.3 g) was dissolved in 0.5 mL of DMF giving a colorless solution. To the solution was added TEMPO (1.08 mmol, 0.17 g). Then, was it added KOH (1.08 mmol, 0.062 g). The reaction was maintained for 24 h until the precipitate formed. The precipitate was separated and a white powder was purified. The liquid phase was treated with acetone and THF until a beige precipitate formed. The products were characterized by EI Mass and IR.

Table 1 summarizes the different reactions that were carried out to determine the effects of using TEMPO, Br-TEMPO, and derivatives of TEMPO. The conditions were chosen according to the observed results from experiments **I** and **II** which indicated that the three reagents 2-methylpropan-2-ol (**1**), trimethylsilanol (**2**), and triphenylsilanol (**3**) did not undergo reaction. The solvent DMF was used due to the very low solubility of (Ph)$_3$SiOH in other solvents. For reactions **II-VIa** a strong base (KOH) was used. Condition **VI**(b) was used the Br-TEMPO and triethylamine in dichloromethane as solvent. Also various derivatives TEMPO were used to prove the reaction occurred with alcohols.

Table 1. Reaction conditions used to evaluate the preparation of the precursor with the

-C-O-O-N- or Si-O-O-N- bond.

	(**1**)	(**2**)	(**3**)
Chemical reagent	$(CH_3)_3COH$	$(CH_3)_3SiOH$	$(Ph)_3SiOH$
Experiment	Conditions used		
I	TEMPO/36-38 °C or 66-68 °C/48 h		
II	TEMPO/DMF/ KOH/36-38 °C/48 h		
III	-	Oxo-TEMPO/ DMF/ KOH/66-68 °C/48 or 24 h	
IV	-	OH-TEMPO/DMF/ KOH/66-68 °C/48 or 24 h	
V	-	NH_2-TEMPO/DMF/ KOH/66-68 °C/48 or 24 h	
VI	(**a**) Br-TEMPO/DMF/KOH/ 36-38 °C and 66-68 °C/48 h	(**b**) Br-TEMPO/CH_2Cl_2/Et_3N /4 °C/4 h	

Crystallization of hexaphenyldisiloxane

In the reactions **II**, **III** and **VI**(b) the crystals of hexaphenyldisiloxane were formed

before the liquid was treated with THF. These crystals were washed with ethanol. The

melting point of crystals was of 225 °C.

X-ray crystallography

All reflection intensities of hexaphenyldisiloxane was measured at 110(2) K using a

SuperNova diffractometer (equipped with Atlas detector) with Cu Kα radiation (λ =

1.54178 Å) under the program CrysAlisPro (Version 1.171.36.32 Agilent Technologies,

2013). The cell dimensions were refined and solved with the program SHELXS-2013

(Sheldrick, 2013) and were refined on F2 with SHELXL-2013.[55] Analytical numeric

absorption corrections based on a multifaceted crystal model were applied using

CrysAlisPro (Version 1.171.36.32 Agilent Technologies, 2013). The temperature of the

data collection was controlled using a Cryojet system (manufactured by Oxford

Instruments). The H atoms were placed at calculated positions using the instructions AFIX

43 with isotropic displacement parameters having values 1.2 times Ueq of the attached C atoms.

Result and discussion

The Br-TEMPO salt was characterized by IR spectroscopy to determine if the characteristic signal for $N^+=O$ was present. To confirm if the Br-TEMPO could oxidize a primary alcohol, we used 1-phenylethanol as a model compound. The IR and ^{1}H-NMR spectra showed the characteristics bands for both the starting material and the oxidized product. The IR and NMR signals were comparable with the reported values and the melting point matched with the expected temperature. The IR spectrum presented the signals characteristic for the acetophenone product in the oxidation reaction, indicating that the TEMPO is in the form of salt. The signal at 1650 cm^{-1} was for νC=O, at 910 cm^{-1} for δC-H in plane and at 775 cm^{-1} for δC-H out-of-plane. The ^{1}H-NMR (CDCl$_3$ ν ppm): s, 2.6 ppm, 3H (CH$_3$), 8 ppm, dd: 2H (o-Ar), 7.45-755 ppm, [m:2H at (m- Ar) and at 7.55 ppm 1H (*para*-H in phenyl group)].

Previous reports had led us to expect that formation of TEMPO-containing alkylsilanes could be difficult.[56] Using the conditions in Table 1, we had an indication that the reaction had taken place by the slight yellow color of the solution due to the consumption of the TEMPO. The characterization of reactions **I** and **II** using 2-methylpropan-2-ol (**1**), trimethylsilanol (**2**), and triphenylsilanol (**3**), indicated that no reaction had occurred because the starting reagents were recovered. However, with reagent (**3**) under reaction conditions **II**, we obtained two white powders, one with a melting point of 225 °C with a yield of 20% and another that did not melt even at temperatures up to >

280 °C, with yield of 80%. The IR, ^{1}H-NMR, EI mass spectrometry characterizations of the powder which melted at 225 °C are showed in Figure 1. The characteristics bands (Figure 1a) were at 3066 and 3016 cm^{-1} and were assigned to νC-H of Ar, δC-H of Ar 1428 cm^{-1} and 1117 cm^{-1}. The signal at 1095 cm^{-1} was assigned to νSi-O-Si,[56] and at 709 cm^{-1} and 515 cm^{-1} were due to νSi-Ph. The ^{1}H-NMR spectrum, Figure 1(b), showed a high degree of symmetry, as indicated by a multiplet with three signals at 7.51-7.49 ppm, 7.42-7.38 ppm, and at 7.30-7.27 ppm for the protons of the aromatic rings. The EI mass spectrum, Figure 1(c), showed the following mass fragments: 457 m/z [$C_{30}H_{25}OSi_2$], 379 m/z [$C_{24}H_{19}OSi_2$], 303 m/z [$C_{18}H_{15}OSi_2$], 257 m/z [$C_{18}H_{15}Si$], 181 m/z [$C_{12}H_{10}Si$], 44 m/z [SiO]. The spectroscopic results showed that the powder was either a di(triphenylsilane)ether or hexaphenyldisiloxane.

It was possible to isolate the product hexaphenyldisiloxane in crystal form and its structure was determined to be an ordered structure. The ORTEP structure of hexaphenyldisiloxane**,** including the atomic numbering scheme is shown in Figure 2, which also includes a view of tridimensional packing. Selected crystal data, the structure solution and refinements are listed in Table 2 and 3.
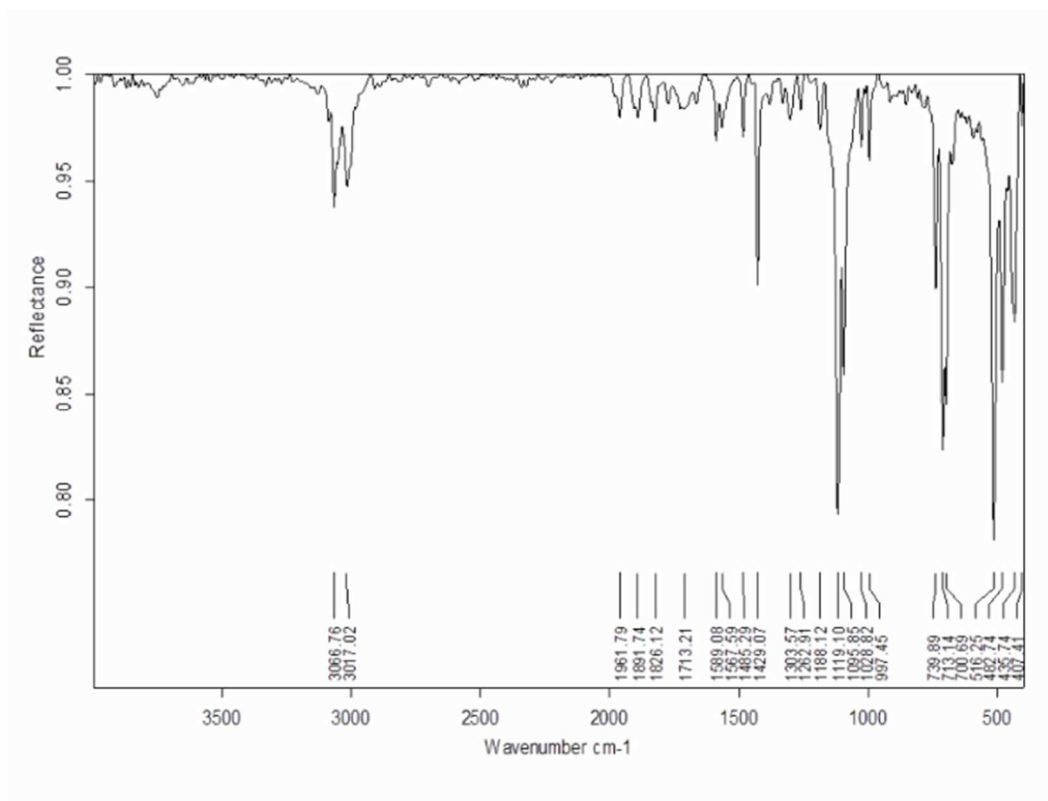
(a)
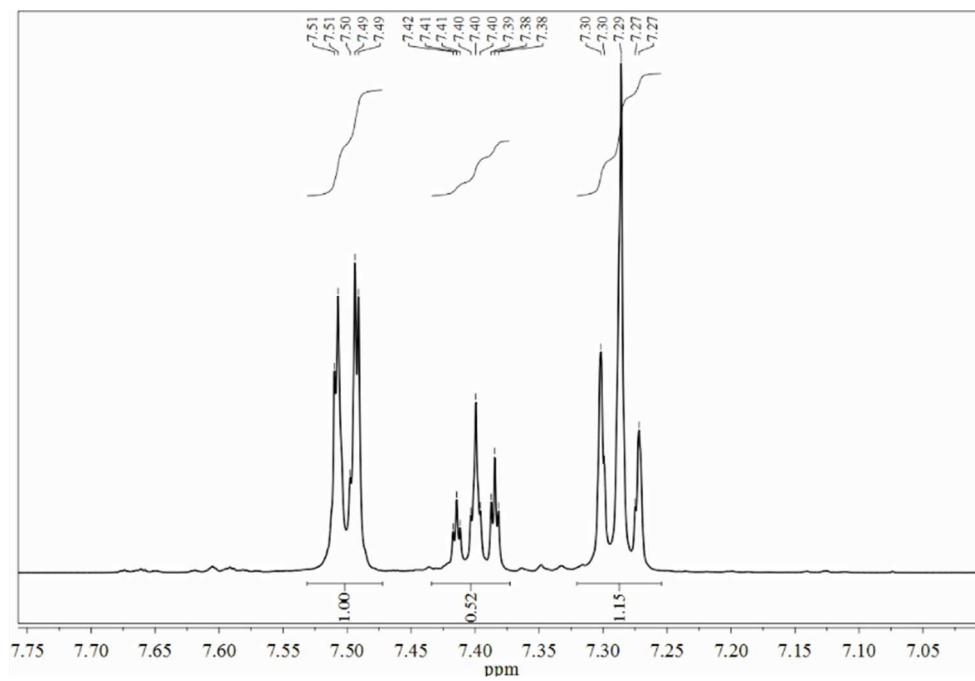
(b)
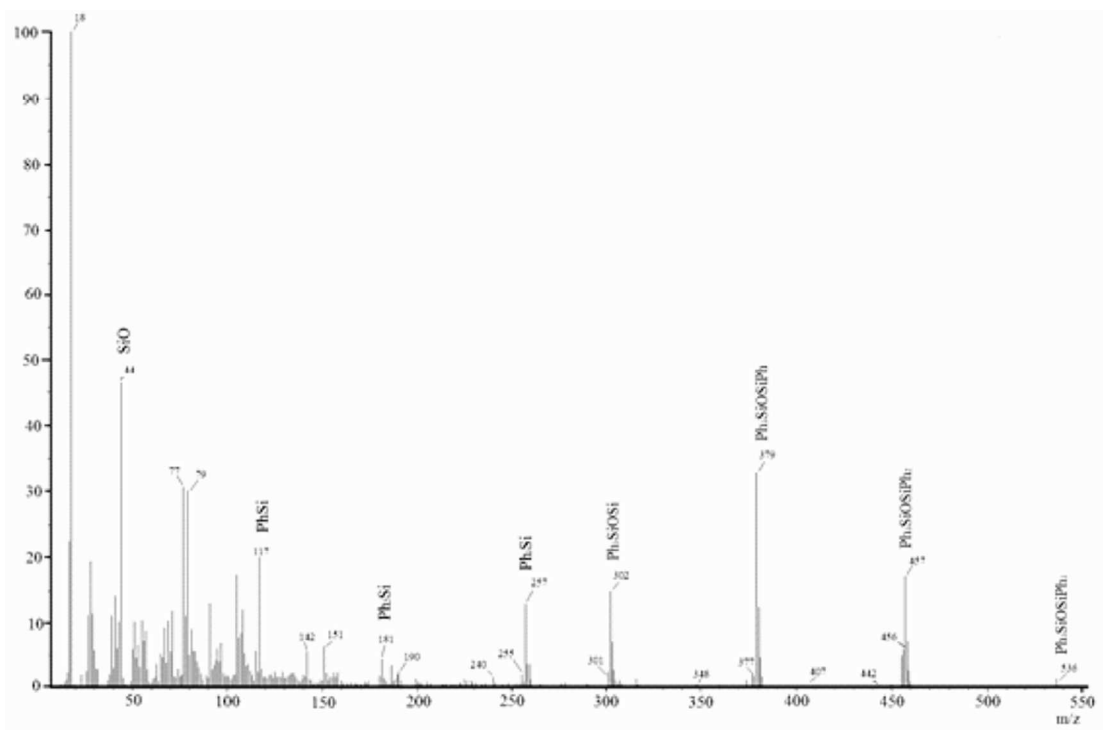
(c)

Figure 1. The IR (a), ^{1}H-NMR (b) and EI mass (c) spectra for the di(triphenylsilane)ether

The molecule belongs to the triclinic system and is of the *P*-1 space group. It has an inversion center through C(1)-O-C(1), C(7)-O-C(7), C(13)-O-C13) of each of the phenyl groups and the central fragment Si--O--Si is linear along the crystallographic c axis. The cell contains Z=1, in contrast to the structure solvated hexaphenyldisiloxane previously reported.[57] The principal interatomic distances are Si(1)---O(1) of 1.6198(3) and 1.6199(3) Å, the Si(1)—C(1)- 1.8692(13) and 1.8654 (13)Å, and Si(1)—O(1) of 1.6198(3) and 1.699(3) finally the S(1)—C of 1.8692 (13)Å, 1.8654(13) and 1.8627(1) for each aromatic ring due to the inversion center. The angle of 180° is indicative of the linearity of the Si(1)—O(1)—Si(1) fragment. Furthermore, angles between O(1)-Si(1)-C(13) of 109.69(4)°, O(1)-Si(1)-C(7) of 108.53(4)° and C(13)-Si(1)-C(7) of 109.80(6)° indicate the tetrahedral geometry of the Si atom.

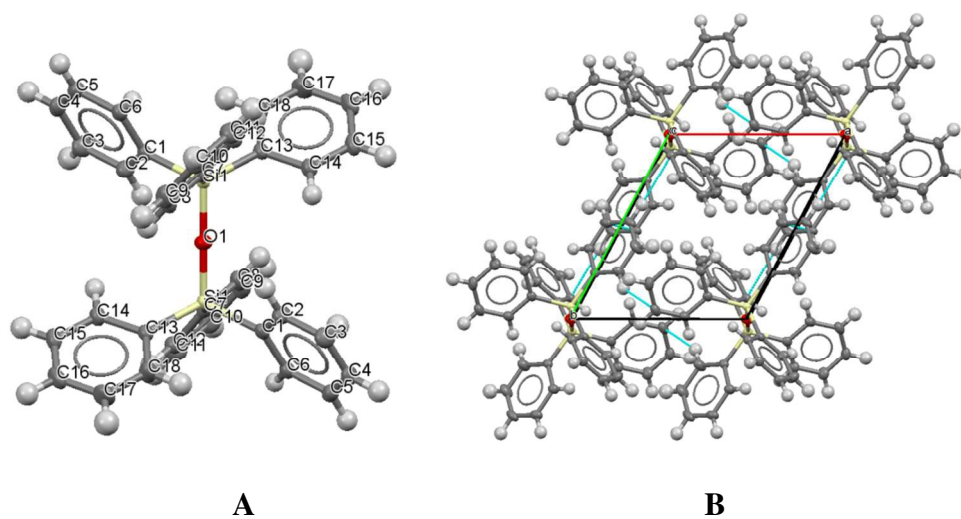A   B

Figure 2. Molecular structure (**A**) of hexaphenyldisiloxane**,** the displacement ellipsoids are drawn at the 50% probability level and H atoms are shown as small spheres of arbitrary radii. (**B**) Stereoscopic view of the packing on the crystallographic c axis.

Table 2. Crystallography Data for hexaphenyldisiloxane

Empirical formula	$C_{36} H_{30} O Si_2$
Crystal system	triclinic
Color, Habit	colorless block
Formula weight	534.78
Space group	*P*-1
T(K)	110(2)
a(Å)	8.5829(4)
b (Å)	9.4856(4)
c (Å)	10.9694(5)
α(°)	95.951(4)
β (°)	90.059(3)
γ (°)	113.352(4
V (Å^3)	727.71(6)
Z	1
Dc(g cm^{-3})	1.220
F (000)	282
μ (mm^{-1})	1.305
λ (Å)	1.54178
Crystal size (mm^3)	$0.31 \times 0.21 \times 0.20$
2θmax(°)	143.8
N	9218
N° (I>2.0 σ(I))	2707
R1	3.18
wR2	8.21
goodness-of-fit	1.046
Largest diff peak and hole (e Å^{-3})	0.49 and -0.27

Table 3. Selected interatomic distances (Å) and angles (°) for hexaphenyldisiloxane

Bond lenght (Å)	
C(1)-Si(1)	1.8692(13)
C(7)-Si(1)	1.8654(13)
C(13)-Si(1)	1.8627(13)
O(1)-Si(1)	1.6198(3)
C(8)-C(9)	1.391(2)
C(10)-C(11)	1.385(2)
Angle bond(°)	
C(12)-C(7)-Si(1)	122.53(10)
C(8)-C(7)-Si(1)	119.86(10)
C(6)-C(1)-Si(1)	120.71(10)
C(2)-C(1)-Si(1)	121.44(10)
C(14)-C(13)-Si(1)	120.17(10)
C(18)-C(13)-Si(1)	122.39(10)
Si(1)-O(1)-Si(1)	180.0
O(1)-Si(1)-C(13)	109.69(4)
O(1)-Si(1)-C(7)	108.53(4)
C(13)-Si(1)-C(7)	109.80(6)
O(1)-Si(1)-C(1)	108.72(4)
C(13)-Si(1)-C(1)	110.30(6)
C(7)-Si(1)-C(1)	109.77(6)

In addition to hexaphenyldisiloxane, the powder with the melting point higher than 280 °C was also obtained with the **III**, **IV** and **V** reaction conditions using reagent (**3**) even though these reactions used derivatives of TEMPO. Only a small difference was observed with the OH-TEMPO. Although this other product was present in small yield, it was possible to characterize it. From the IR spectrum (Figure 3) we observed the signal at 1428 cm^{-1} assigned to Si-C(Ph) which was reported as a sharp and intense band (1430 cm^{-1});[57] the band at 1117 cm^{-1} is also due to the presence of a νSi-C(Ph), but the new band at 1095 cm^{-1} (which was not present in the spectra of the starting reagents), could be due to the Si-O. The three bands in the range of 760-710 cm^{-1} of approximately equal intensity are typical for the presence of Si-phenyl. The difference in the spectrum for the ether

16

compound was the signal at 1350 cm^{-1}, which in TEMPO has been reported to correlate with the C-N in the range of 1250–1000 cm^{-1} (m). For OH-TEMPO, a band appeared at 1350 cm^{-1} corresponding to C-N, as well as another broad band at 1590 cm^{-1}. We questioned if these bands gave evidence of the presence of Si-O-N bond?
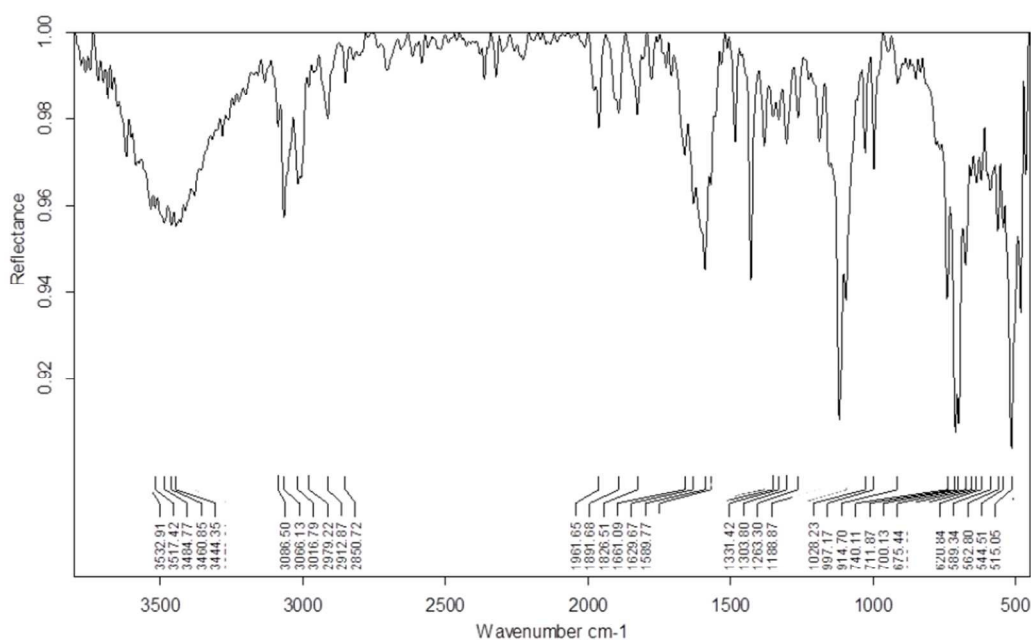

Figure 3. IR spectrum for silaneoxiamine compound

In order to identify better the signals was performed theoretical calculations of the fully optimized structures of the compound with moieties Si-O-Si and Si-O-N. The calculations were carried out using DFT calculations with the hybrid functional B3LYP,[58] with the basis set 6-311++G(d,p),[59] in the Gaussian09 computational package.[60] For calculations, the initial guess of the system (hexaphenyldisiloxane) was obtained from X-ray coordinates data, while for system (triphenylsilaneoxiamine) was computationally built. Vibrational frequencies of both compounds were calculated at the same level of theory in gas phase and including the effect of *n,n*-dimethylformamide (DMF) with ε=37.219 using

17

the Polarizable Continuum Model (PCM).[61] The selected parameters are shown in Table 4. The effect of the solvent DMF was not significant on the structural parameters. Geometry parameters obtained in gas phase MP2/6-31G(d) calculations were in good agreement with the parameters for hexaphenyldisiloxane, see Table 3. For Si-O-N compound good results were obtained in comparison to other siliceoxiamine systems containing Si-O-N fragments in its structure. Geometry parameters obtained in gas phase MP2/6-31G(d) calculations were Si–O= 1.623(3) Å, O–N= 1.479(6) Å and Si–O–N= 105.6(8)° reported in reference for $Cl_3SiONMe_2$ compound.[62] The structures of $H_3SiONMe_2$ and $H_2Si(ONMe_2)_2$ showed parameters of Si–O= 1.682 and 1.699 Å, O–N= 1.459 and 1.477 Å, and Si–O–N= 102.5 and 94.2, respectively,[63] while $ClH_2SiONMe_2$ showed Si–O= 1.678 Å, O–N= 1.468 Å and Si–O–N= 91.6° in MP2/6-311G(d,p).[64] Parameters of $H_3SiON(BH_3)Me_2$, $FH_2SiON(BH_3)Me_2$ and $H_3SiOC(CH_3)Me_2$ were calculated at MP2/6-311G(d,p) level of theory, obtaining similar values to those previously reported (Si–O= 1.707, 1.700 and 1.657 Å, O–N= 1.433 and 1.428 Å and Si–O–N= 121.4 and 119.7°).[65] For $F_3SiONMe_2$ calculated values at MP2/6-311G(d,p) level of theory were reported with values of Si–O= 1.626 Å, O–N= 1.478 Å and Si–O–N= 103.5°.[66]

For the compounds containing Si-O-N fragments N··Si interaction has been calculated in the range of 1.963–2.768 Å,[61-65] which indicate a intramolecular donor-acceptor interaction between silicon and nitrogen, leading to noticeably narrow Si-O-N angles (at range of 82.9-113.2°) for systems containing pyrrole, pyrrolidine and piperidine groups.[67] More recently, one structure containing TEMPO-SiCl$_3$ was characterized crystallographically and using DFT calculations.[68] In this work, authors reported similar characteristics parameters Si–O= 1.638 Å, O–N= 1.469 Å, N··Si=2.748 and Si–O–N=

124.3° for their compound TEMPO-SiCl$_3$ which contains the similar fragment Si–O–N,

showed structural features that gave an indication of possible presence of the Si-O-N bonds,

that corresponding to a silaneoxiamine, Table 4. Figure 4 shows the optimized structures

with moieties Si-O-Si and Si-O-N calculated at B3LYP/6-311++G(d,p) theory level.

Table 4. Theoretical B3LYP/6-311++G(d,p) selected structural parameters of the optimized

structures with moieties SiOSi and SiON. Internuclear distances in (Å), and valence

angles in (º).

Parameter	Si-O-Si		Si-O-N	
	Gas	DMF	Gas	DMF
Si–O	1.64983	1.65023	1.69395	1.69336
Si–C	1.88638	1.88749	1.89287	1.89432
N–O	----	----	1.45801	1.45983
C–N	----	----	1.50345	1.50394
C=C	1.39337	1.39423	1.39228	1.39311
C–C	----	----	1.54654	1.54682
C$_{Ph}$–H	1.08560	1.08547	1.08580	1.08582
C–H	----	----	1.09464	1.09437
Si–O–Si	180.00000	180.00000	----	----
Si–O–N	----	----	124.05473	124.28608
C–Si–O	108.49329	108.57186	111.42343	110.81206
C–C–Si	120.34040	120.42375	119.37505	119.32609
C–Si–C	110.43251	110.36428	109.70218	110.12654
C–N–O	----	----	107.92266	108.01966
C–N–C	----	----	118.23619	118.34112
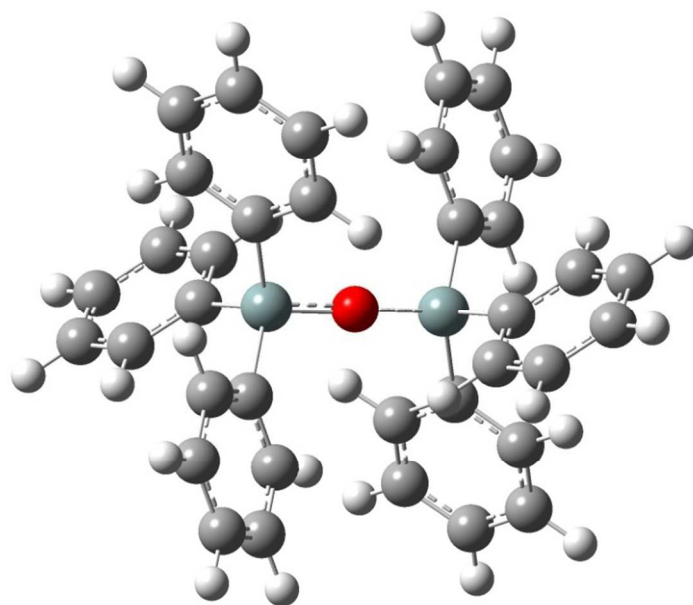
hexaphenyldisiloxane
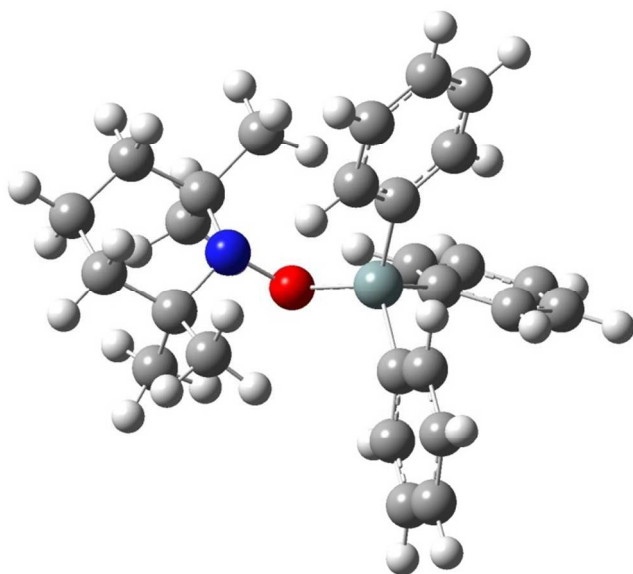
triphenylsilaneoxiamine

Figure 4. Optimized structures with moeties Si-O-Si and Si-O-N calculated at B3LYP/6-311++G(d,p) theory level.

On the other hand, the vibration wavelengths form theoretical calculations are resumed in Table 5. Stretching vibrations Si-O were found at 1088.56 and 1076.98 cm^{-1} for compound hexaphenyldisiloxane and at 832.02 and 828.01 cm^{-1} for compound triphenylsilaneoxiamine, in gas and solvent phases, respectively. Bending vibrations of Si-O were located at 527.8 and 519.1 cm^{-1} for hexaphenyldisiloxane in the gas and solvent phases, while for triphenylsilaneoxiamine, two bending vibrations are located at 517.92 and 527.25 cm^{-1} in gas phase and at 512.27 and 522.60 cm^{-1} in solution, due to the non-symmetrical structure of triphenylsilaneoxiamine compound in comparison to hexaphenyldisiloxane structure. In early work,[69] an IR band appeared at 1080 cm^{-1} for the Si-O-Si bond for the formation of a gel of silica. In this work, Orcel et al. indicated the absorption bands due to the silica network were located between 1100 and 800 cm^{-1} and the deformation of the Si-O-Si appeared at 455 cm^{-1}. The vibrational frequencies in the IR spectra have been reported for compounds with bridged Si-O-Si groups,[70] which are in agreement, to a certain degree, according to the silicon precursor (Table 5). For the triphenylsilaneoxiamine compound, several vibrational frequencies were in agreement with those assigned for TEMPO compound (Table 5). [71]

Furthermore, the ^{1}H-NMR and EI mass spectra (Figures 5 and 6) showed that presence of triphenylsilane and OH-TEMPO. The m/z resulting fragmentation gave the EI mass spectrum, which indicated the presence of the silaneoxiamine moiety, Figure 6. However, the ether compound always was obtained in greater yield in almost all reactions performed and a very little yield the corresponding the silaneoxiamine, even though the reaction was performed with the reaction conditions reported.[53]
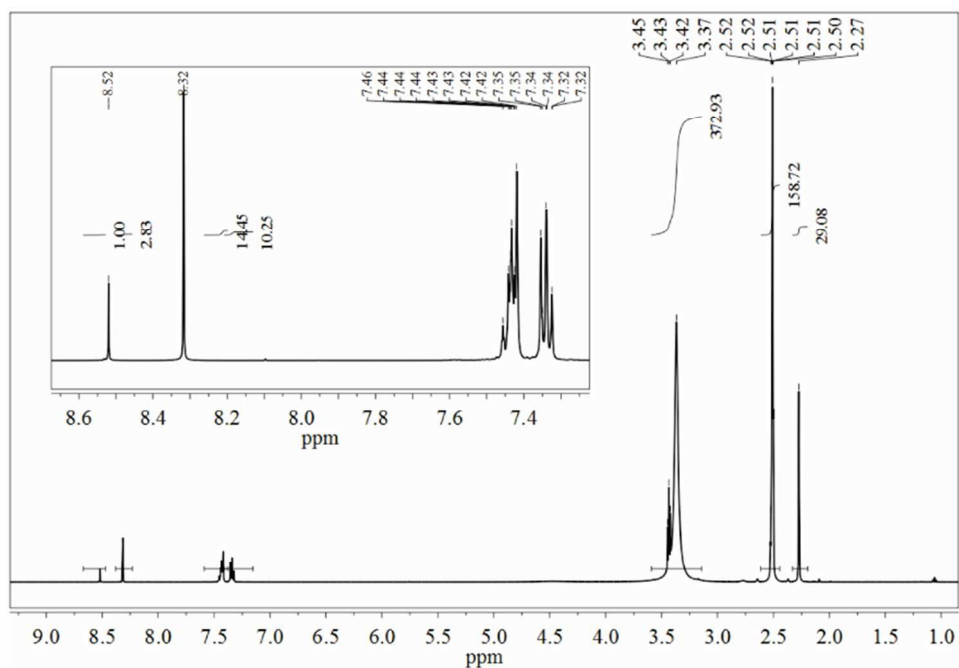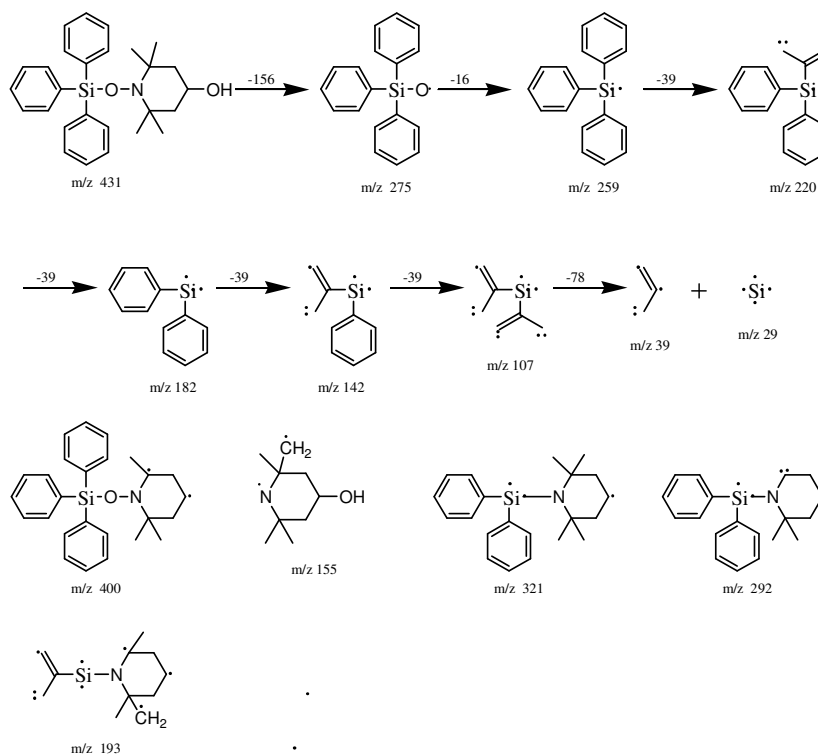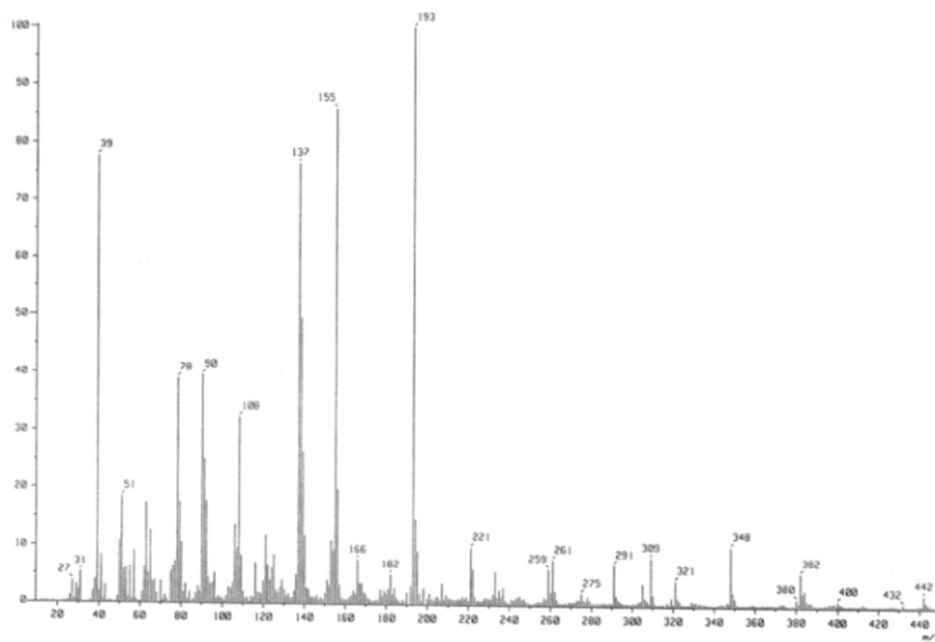
Figure 5. ^{1}H-NMR spectrum for silaneoxiamine

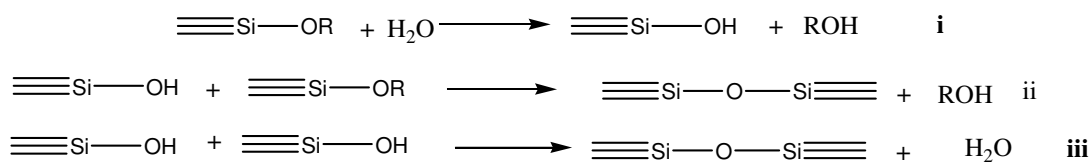Figure 6. EI mass spectrum and proposed fragmentation for silaneoxiamine

Table 5. Theoretical B3LYP/6-311++G(d,p) vibrational frequencies in (cm^{-1}) of the optimized structures with moieties Si-O-Si and Si-O-N in gas phase and solvent DMF phases. Vibrational frequencies of TEMPO are included by sake of comparison at the same level of theory.

Band (cm^{-1})	Structural unit	Hexaphenyldisiloxane		Triphenylsilaneoxiamine		TEMPO	
		Gas	DMF	Gas	DMF	Gas	DMF
δ(Si-O)	Si-O-Si	527.78	519.00	517.92	512.27	----	----
		527.84	519.25	527.25	522.60	----	----
δ(C-H)wagging	-CH$_2$, -CH$_3$	----	----	----	----	530.96	528.49
δ(N-C)wagging	C-N-C	----	----	556.00	553.61	550.78	549.80
δ(N-O)bending	C-N-O	----	----	687.12	685.45	629.63	627.73
δ(C-H)wagging	-Ph	714.74	713.59	711.74	711.93	----	----
		714.92	713.81	713.33	713.08	----	----
		715.79	714.15	715.00	714.33	----	----
δ (C-C)ring puckering	-Ph (five adjacent H)	722.13	717.92	717.66	715.49	----	----
		722.17	718.03	721.77	718.81	----	----
δ(C-H)wagging	-Si-Ph	753.62	752.95	750.74	750.35	----	----
		758.20	758.12	755.81	758.16	----	----
		758.24	758.20	758.32	758.92	----	----
ν(N-O)	-N-O	----	----	952.21	943.86	----	----
ν(Si-O)asym	-Si-O-Si, Si-O	1088.56	1076.98	832.02	828.01	----	----
δ(C-H)rocking	-CH$_2$, -CH$_3$	----	----	968.40	966.69	968.86	967.94
		----	----	984.79	982.51	983.24	981.36
		----	----	1063.99	1061.56	1060.88	1058.96
ν(Si-C)asym	Si-Ph	1121.07	1118.29	1116.95	1114.72	----	----
		1130.04	1126.98	1124.61	1121.47	----	----
		1130.19	1127.20	1127.20	1124.88	----	----
δ(C-H)twisting	-CH$_2$	----	----	1149.74	1146.55	1144.61	1141.18
δ(C-C)bending	Ring vibration	----	----	1202.41	1198.83	1195.68	1190.15
δ(C-C)wagging	Ring vibration	----	----	1226.66	1224.31	1213.93	1211.78
ν(C-C)sym	-C-CH$_2$	----	----	1259.27	1256.45	1265.15	1258.35
ν(C-N)asym	C-N-C	----	----	1280.27	1276.67	1276.67	1271.54
ν(C-C)sym	-Ph	1299.59	1296.91	1298.50	1295.66	----	----
		1302.48	1299.32	1300.39	1297.73	----	----

		1302.57	1299.46	1304.08	1300.87	----	----
ν(NO$^{\bullet}$)	-NO$^{\bullet}$	----	----	----	----	1372.90	1372.3
δ(C-H)wagging	-CH$_2$	----	----	1379.71	1377.07	1390.22	1388.21
		----	----	1395.95	1390.60	1395.84	1393.34
δ(C-H)wagging	-CH$_3$	----	----	1412.66	1405.73	1413.31	1406.67
		----	----	1417.28	1409.59	1422.35	1417.08
δ(C-H)bending	-Ph	1457.10	1455.12	1456.35	1454.00	----	----
		1457.94	1455.47	1457.47	1455.36	----	----
		1457.96	1455.81	1459.02	1456.80	----	----
δ(C-H)twisting	-CH$_3$	----	----	1493.54	1484.39	1499.64	1489.27
		----	----	1505.36	1498.56	1507.69	1499.58
		----	----	1510.54	1504.23	1511.17	1498.95
δ(C-C)bending	-Ph	1515.68	1513.75	1515.78	1513.65	----	----
		1516.60	1514.34	1517.16	1515.14	----	----
		1516.78	1514.51	1517.44	1516.23	----	----
ν(C-C)asym	-Ph	1606.12	1602.60	1605.65	1602.12	----	----
		1606.88	1603.06	1606.54	1602.91	----	----
		1606.94	1603.18	1607.11	1603.53	----	----
ν(C-C)sym	-Ph	1628.29	1624.38	1628.01	1623.94	----	----
		1628.84	1624.83	1628.72	1624.62	----	----
		1628.86	1624.94	1629.03	1625.01	----	----
ν(C-H)asym	-CH$_2$	----	----	3051.80	3053.99	3056.25	3061.61
		----	----	3056.69	3057.76	3056.69	3062.34
		----	----	3066.73	3066.99	3066.57	3069.55
ν(C-H)sym	-CH$_2$	----	----	3015.62	3015.26	3014.31	3017.06
		----	----	3017.78	3016.03	3015.46	3018.22
		----	----	3026.36	3027.43	3027.36	3030.10
ν(C-H)asym	-CH$_3$	----	----	3100.81	3099.97	3097.40	3098.91
		----	----	3103.65	3102.46	3099.25	3101.77
		----	----	3110.34	3108.85	3103.12	3104.36
ν(C-H)sym	-CH$_3$	----	----	3129.01	3122.19	3115.43	3112.40
		---	---	3140.09	3137.76	3119.92	3119.66
		----	----	3143.15	3140.21	3132.03	3125.42
ν(C-H)asym	-Ph	3164.86	3166.59	3167.12	3168.96	----	----

| v(C-H)sym	-Ph	3164.90	3166.67	3169.55	3171.15	----	----
		3165.15	3166.83	3169.55	3173.32	----	----
		3173.40	3174.47	3175.17	3176.35	----	----
		3173.44	3174.48	3181.18	3180.46	----	----
		3173.47	3174.54	3181.55	3183.23	----	----
		3183.58	3185.49	3183.94	3185.85	----	----
		3183.60	3185.56	3187.80	3187.63	----	----
		3183.78	3185.75	3193.46	3194.62	----	----

The sol-gel process is a well-known method for converting chemical precursors into ceramics and glasses with the desired properties. The process can produce a wide range of compositions (mostly oxides) in various forms, including powders, fibers, coatings and thin films, monoliths and composites, and porous membranes.[70, 73-75] By controlling the synthesis conditions carefully, sol morphology can be directed towards branched polymeric systems or toward particulate systems.[73] Control of relative rates of hydrolysis and polycondensation, the respective mechanism (Scheme 4), as well as the factors of pH, process temperature, pressure, solvent, concentration of alkoxide, type and concentration of catalysts and DCCA (Drying Control Chemical Additive), play important roles in determining morphology of the resulting polymeric structure.[73,74,76] Besides the possibility of modifying the hydrolysis and polycondensation reactions, it is now well known that addition of DCCA to a mixture of alkoxide, water, and alcohol improves the processing control of gel structures and processability.[76-80] The sol-gel process of silica involves the hydrolysis [i] and condensation [ii, iii] of alkoxides, such as tetraethoxysilane or tetramethoxysilane. These monosilanes form in these reactions [i-iii] various diverse linear, branched and cyclic intermediates (Scheme 4).[73-76]

$$\equiv Si-OR + H_2O \longrightarrow \equiv Si-OH + ROH \qquad \textbf{i}$$

$$\equiv Si-OH + \equiv Si-OR \longrightarrow \equiv Si-O-Si\equiv + ROH \quad \text{ii}$$

$$\equiv Si-OH + \equiv Si-OH \longrightarrow \equiv Si-O-Si\equiv + H_2O \qquad \textbf{iii}$$

Scheme 4. Hydrolysis and polycondensation mechanism

The compounds as powder white, which was obtained in good percentage in the reactions **II-IV** (for **3**) and for the reagent (**2**) at reactions conditions **V**(a) with a melting point > 280 °C, could be due to process that carried out during the funtionalized, i.e. the

formation of an oxide network or in linear chain through polycondensation reactions of a molecular precursor (hexaphenyldisiloxane) that is formed in situ, Scheme 5.
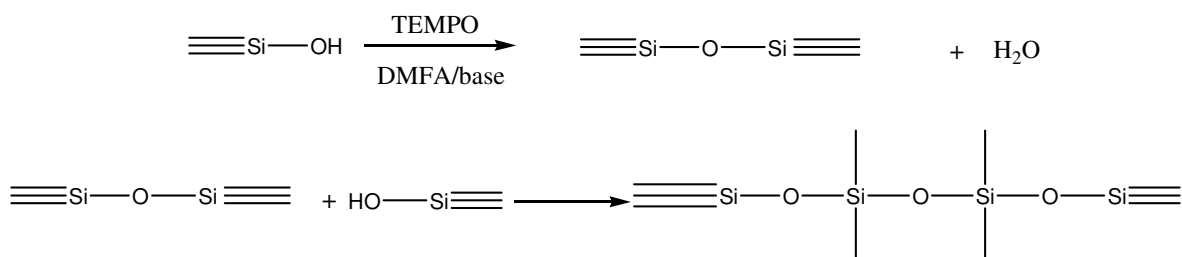
Scheme 5. Proposed mechanism to form a silica oxide.

The characterization was made for IR, Figure 7 shows the spectra for products from the reactions of **2** at conditions of **VI**(a) (Figure 7i) and **3** at **II** (Figure 7ii). In Figure 7i, the bands are broad, which is an indication of a polymer type structure. The principal signals at 1095 cm^{-1} and 514 cm^{-1} assigned to νSi-O-Si and δSi-O for the ether forms are missing. The signal at 704 cm^{-1} was assigned to δ(C-H) wagging and at 1416 cm^{-1} is due to δC-H of Si-Ph according to reference.[71] The new signals for the Si-O(H) stretching band around of 982 cm^{-1} and one due to Si-O of $\equiv$Si-OH, for reagent triphenylsilanol appeared at 856 cm^{-1}. The band at around 915 cm^{-1} was associated with non-bridging free broken Si-O bonds.[71] Spectrum analysis revealed the bands at 833, 665, 598, 481 and 424 cm^{-1} that corresponded to νSi-C (Si-R), νSi-O-Si (structural unit $\equiv$Si-O-Si$\equiv$), νSi-O (SiO$_2$) defect, and the important unit, the -O-Si-O- bond for the formation of a gel of silica.[70,71] The spectrum also presented a strong band at about 1662 cm^{-1} characteristic of a C=O bond which, belonging to formate or amide groups, was present in the spectra of sols containing formamide, since formamide is a typical DCCA, as shown for previous studies.[74-76]
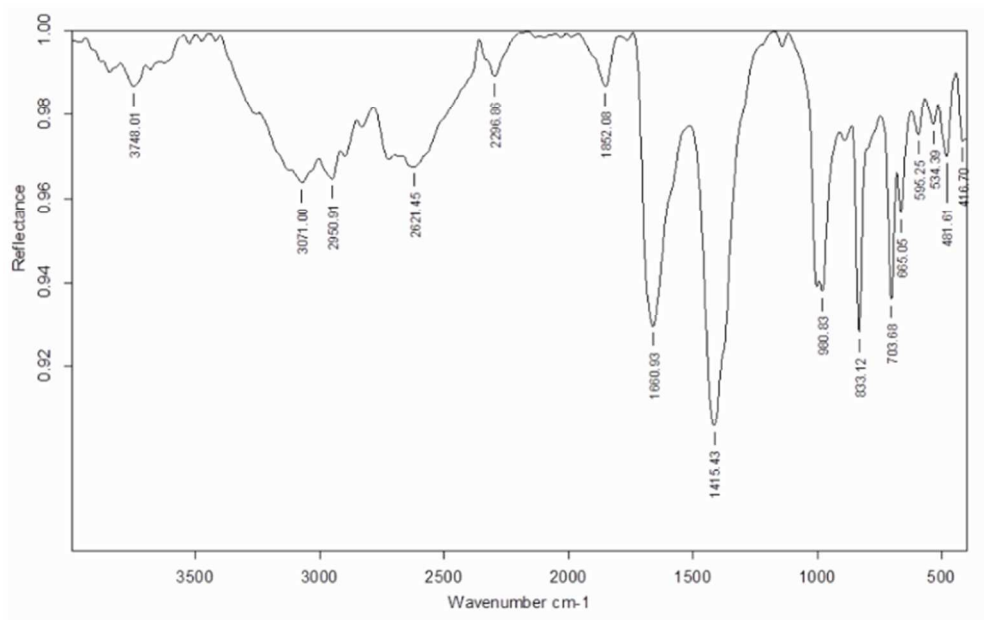
(**i**)
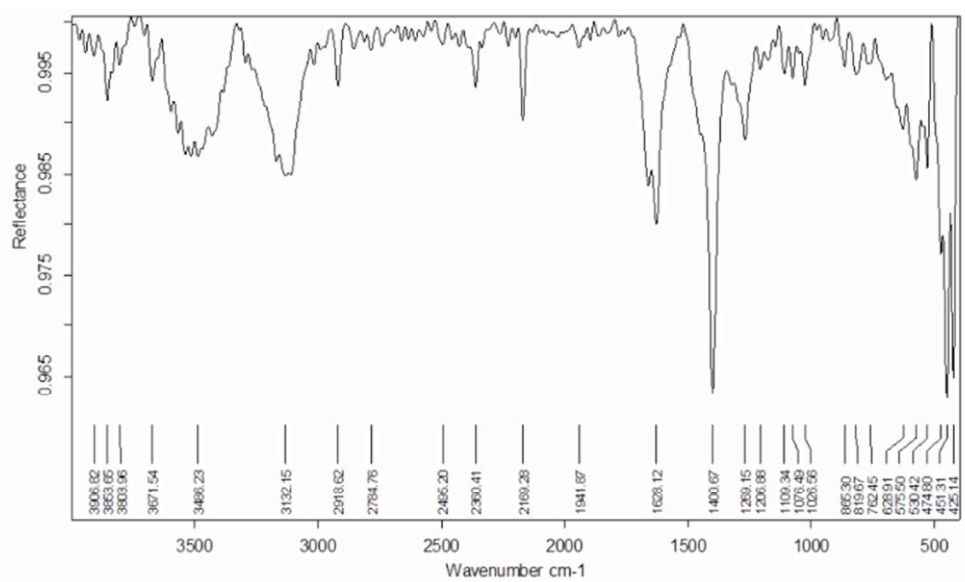
(**ii**)

Figure 7. The IR spectra from reactions 2 at **V**(a) (**i**) and 3 at **II** (**ii**).

Finally, in the IR spectrum of the product obtained from the reaction carried out with trimethylsilanol (Figure 7b), the νSi-CH$_3$ was assigned at 1269 cm^{-1}, the band at 865, 819 and 726 cm^{-1} corresponded to the weak band in polysiloxanes. We did not observe the presence of a band for C=O corresponding to an amide as for the **II** reaction. The IR

spectrum of the sample exhibited a characteristic broad band at 3486 cm^{-1} corresponding to molecular water hydrogen-bonded to each other and to Si-OH groups. The 1630 cm^{-1} peak was due to the vibration of molecular water.[75,79,80] The following Figure 8 shows the EI mass spectrum and fragmentation diagram m/z that allowed us to propose the structure as approximately n=8 units of -($\equiv$Si-O)$_n$-.
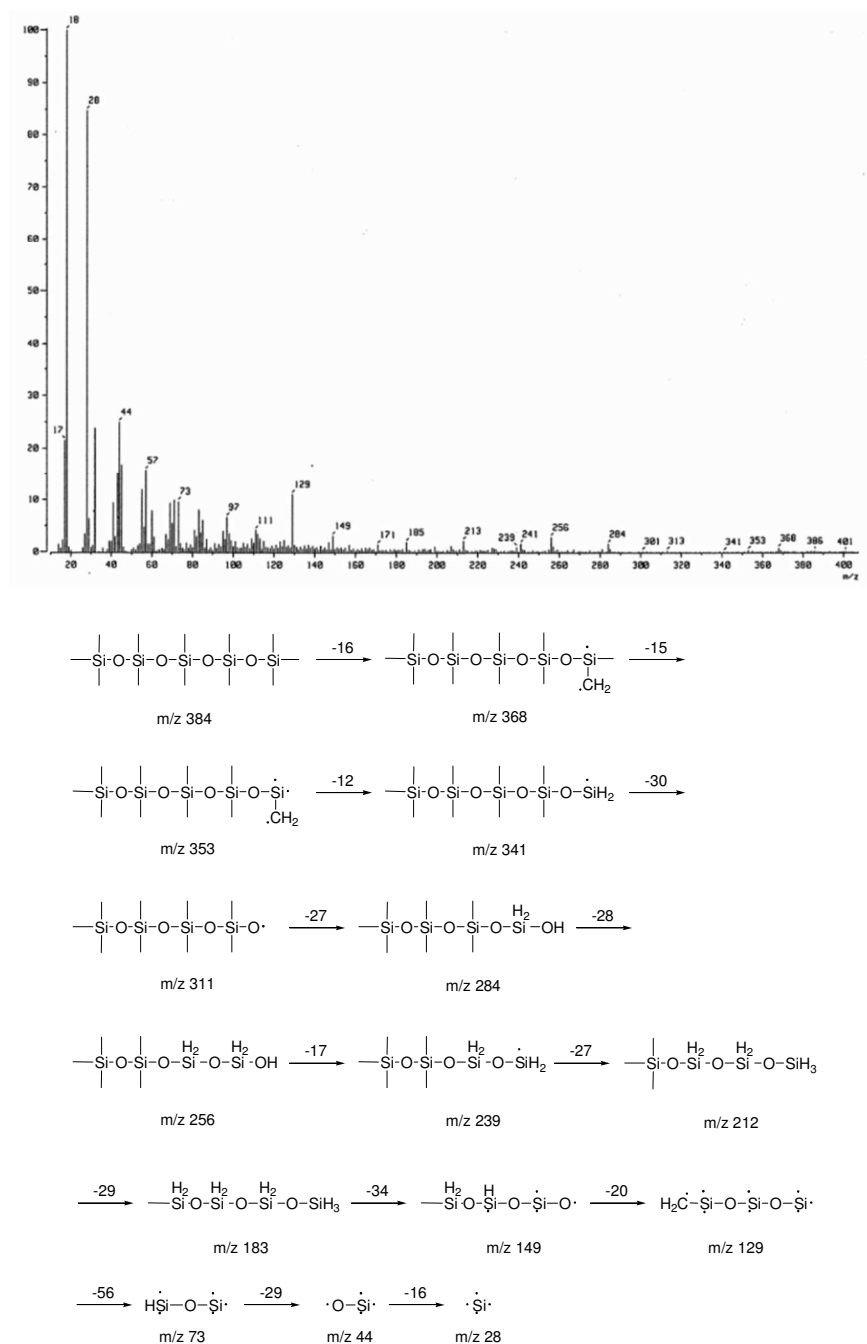

Figure 8. Compound IR spectrum and proposed fragmentation for the reaction 3 at **II**

30

Surprisingly, Figure 9a shows semi-rectangular morphologies obtained in the sample of the reaction **3** at **II**. Here, we proposed that the presence of nitroxide radicals could provide some control during the reaction to produce solid structures with regular shape and size. Figure 9a reaffirmed our proposed mechanism (see Scheme 5) which is in agreement with mass analysis. TEMPO radicals can catalyze the –OH from silanol groups to obtain a network of siloxane groups. Also, these new structures do not have a melting point as revealed in Figure 9b, confirming that the structures are very stable up to 380 °C, which must be due to the Si-O-Si bonds formed by dihydroxylation as catalyzed by TEMPO.
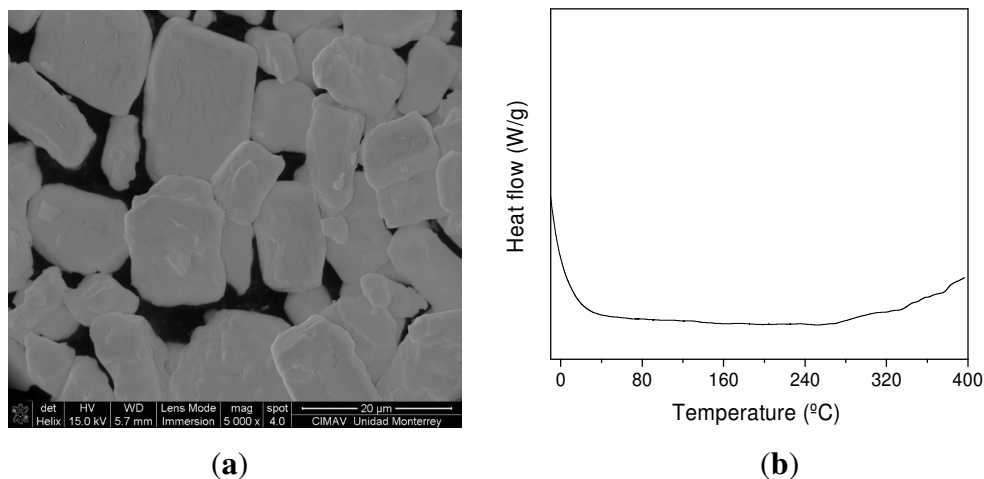

(**a**)   (**b**)

Figure 9. Micrography adquired by SEM (**a**) and thermogram recorderd by DSC (**b**) of compound of the reaction **3** at **II**.

Conclusions

The results of our study showed that it is possible to elucidate which kind of product

will be present when the functionalization of silanol model compounds is carried out with

TEMPO, Br-TEMPO or TEMPO derivatives. Therefore, the surface of organo-modified

silica could be a combination of the diverse silicon materials present (Scheme 6). Also, the

reaction conditions using TEMPO/DMF/base affect the Si-O-Si moiety and structures type

-(≡Si-O)n- due to a reaction that proceeds *in situ*. Reaction with Br-TEMPO/weak base

provided only Si-O-Si moiety, and with OH-TEMPO, the Si-O-N- and -(≡Si-O)n were

formed. Thus, the activity of the functionalization of silica could be based on the quantity

of groups that affect its final properties in the product. The synthetic method reported

herein indicated that is possible to control the chain or network of a Si-O-Si bonds. The

results show that hexaphenyldisiloxane and silaneoxiamine were obtained using TEMPO,

indicating that Br-TEMPO has little effect in the functionalization of silica nanoparticles.

Also, DFT theoretical calculations let us detect the triphenylsilaneoxiamine compound

presents the characteristic interaction N···Si as the compounds containing Si-O-N fragments.

This intramolecular donor-acceptor interaction between silicon and nitrogen provides

narrow Si-O-N angles, which were found adequately from calculations. On the other hand,

the vibrational frequencies calculations were useful for the complete characterization of

hexaphenyldisiloxane and triphenylsilaneoxiamine compounds. Characteristic stretching

vibrations Si-O, Si-N, Si-C, N-O and N-O$^\bullet$ were analyzed from calculations in order to

discern in the formation of the bonds Si-O-Si and Si-O-N in both molecular structures.

Therefore, theoretical calculations could be important in the characterization of systems

containing silica, otherwise difficult to analyze. These outcomes open different researches

on the silica functionalization using interesting processes.
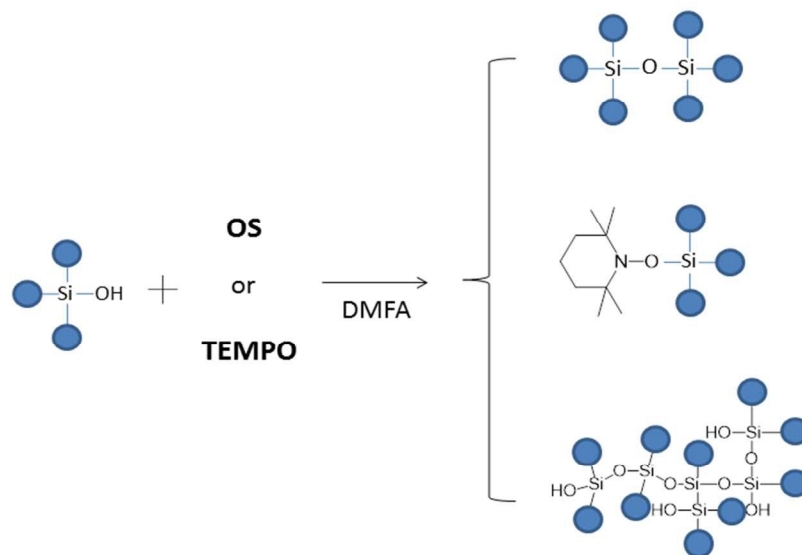
Scheme 6. Depiction of methyl or phenyl groups, with newly formed Si-O-Si bonds at the silane/SiO_2 interface or Si-O-N-extending the SiO_2 network.

Supplementary Material. Crystallographic data (excluding structure factors) reported in this paper have been deposited with the Cambridge Crystallographic Data Centre as supplementary publication no. CCDC 1064074. Copies of available material can be obtained, free of charge, on application to the CCDC, 12 Union Road. Cambridge CB2 IEZ, UK, (fax: +44-(0)1223-336033 or e-mail: deposit@ccdc.cam.ac.uk).

RSC Advances Accepted Manuscript

References

[1] G. Koerner, M. Schulze and J. Weis (eds), Silicones: chemistry and technology, Vulkan-Verlag, Essen, Germany, 1991.

[2] M. Engel, B. Hisgen, R. Keller, W. Kreuder, B. Reck, H. Ringsdorf, H.-W. Schmidt and P. Tschirner, Synthesis, structure and properties of liquid crystalline polymers, *P. Pure Appl. Chem.*, 1985, **57**, 1009–1014.

[3] Z.-Q. Zang, Y.-F. Luo, D. Zhang, X.-H. Wan and Q.-F. Zhou, Synthesis of novel liquid crystalline poly(meth)acrylates containing siloxane spacer and terphenylene mesogenic unit, *Chin. J. Poly. Sci.*, 2000, **18**,101–107.

[4] Y. Kawakami, H. Inoue, N. Kishimoto and A. Mori, Synthesis and characterization of liquid crystalline polystyrenes with disiloxane linkage in the spacer, *Polym. Bull.* 1996, **36**, 653–658.

[5] M. Reihmann, A. Crudeli, C. Blanc, V. Lorman, Y. P. Panarin, J. K. Vij, N. Olsson and G. Galli, Structure and properties of new de vries SmA* liquid crystals, *Ferroelectrics* 2004, **309**, 111–119.

[6] M. Ibn-Elhaj, A. Skoulios, D. Guillon, J. Newton, P. Hodge and H. J. Coles, Structural characterization of new ferroelectric liquid-crystalline siloxanes, *J. Phys. II France* 1996, **6**, 271–279.

[7] C. T. Imrie and P. A. Henderson, Liquid crystal dimers and higher oligomers: between monomers and polymers, *Chem. Soc. Rev.* 2007, **36**, 2096–2124.

[8] R. R. Levier, M. L.Chandler and S. R. Wendel, The pharmacology of silanes and siloxanes. In the biochemistry of silicon and related problems, G. Bendz, and I. Lindquist, Eds.Plenum: New York, 1978, 473.

[9] B. Sander, The value and new directions of silicon chemistry for obtaining bioactive compound in silicon chemistry, J. Y. Cory and E. R. Corey, Eds. Ellis Horwood Ltd. England, 1988, 135–144. Chapter 13.

[10] S. Napier, S. M. Marcuccio, H. Tye and M. Whittaker, A robust method for the Hiyama-type coupling of arylsiloxanes and disiloxanes with aryl halides, *Tetrahedron Lett.* 2008, **49**, 3939–3942.

[11] H. F Sore, C. M.Boehner, S. J. F. MacDonald, D. Norton, D. J. Fox and D. R. Spring, Fluoride-free cross coupling using vinyldisiloxanes, *Org. Biomol. Chem.* 2009, **7**, 1068–1071.

[12] W. T. Grubb, A rate study of the silanol condensation reaction at 25 ° in alcoholic solvents, *J. Am. Chem. Soc.* 1954, **76**, 3408–3414.

[13] M. Sridhar, B. C. Ramanaiah, C. Narsaiah, M. K. Swamy, B. Mahesh and M. K. K. Reddy, An efficient and simple method for the preparation of symmetrical disiloxanes from hydrosilanes by Lewis acid-catalyzed air oxidation, *Tetrahedron Lett.*, 2009, **50**, 7166-7168.

[14] G., Maass, H. J. Lucking, W. Buchner and B. Degen, U.S. Patent 4,060,537, 1977.

[15] T. Minoru, S. Toshio and N. Yoshiaki, G.B. Patent 1,435, 465, 1976.

[16] R. K. Iler, The chemistry of silica. New York: Wiley, 1979.

[17] R. P. W. Scott, Silica gel and bonded phases. New York: Wiley, 1993.

[18] H. E. Bergna, The colloid chemistry of silica, vol. 234. Washington DC, American Chemical Society, 1994.

[19] D. W. Sindorf and G. E. Maciel, Solid-state NMR studies of the reactions of silica surfaces with polyfunctional chloromethylsilanes and ethoxymethylsilanes, *J. Am. Chem. Soc.* 1983, **105**, 3767–3776.

[20] G. E. Maciel, C. E. Bronnimann, R. S. Zeigler, J. S. Chuang, K. R. Kinney and E. A. Keiter, The colloid chemistry of silica. Washington, DC: American Chemical Society, 1994. 260.

[21] A. M. Zaper and J. L. Koenig, Application of solid state carbon-13 NMR spectroscopy to chemically modified surfaces, *Polym. Composite* 1985, **6**, 156–161.

[22] B. Arkles, Tailoring surfaces with silanes, *Chemtech* 1977, **7**, 766–778.

[23] B. Arkles, Gelest 2000, Copyright Glest, Inc., Tullytown, PA, 1988, 16–104.

[24] J. H. Clarkand D. J. Macquarrie, Catalysis of liquid phase organic reactions using chemically modified mesoporous inorganic solids, *Chem. Commun.* 1998, **8**, 853–860.

[25] H. L. Frisch, J. M. West, C. G. Göltner and G. S. Attard, Pseudo IPNs and IPNs of two porous silicas and polystyrene, *J. Polym. Sci., Part A, Polym Chem*, 1996, **9**, 1823–1826.

[26] C. J. T. Landry, B. K. Coltrain, D. M. Teegarden, T. E. Long and V. K. Long, Use of organic copolymers as compatibilizers for organic–inorganic composites, *Macromolecules*, 1996, 29, 4712–4721.

[27] U. Deschler, P. Kleinschmit and P. Panster, 3-Chlorporpyltrialkoxysilane – Schlüsselbausteine für die industrielle Herstellung organofunktionalisierter Silane und Polysiloxane sowie moderner Verbundmaterialien, *Angew. Chem.* 1986, 98 237–253.

[28] P. Fontaine, D. Goguenheim, D. Deresmes, D.Vuillaume, M. Garet and F. Rondelez, Octadecyltrichlorosilane monolayers as ultrathin gate insulating films in metal-insulator-semiconductor devices, *Appl. Phys. Lett.* 1993, **62**, 2256–2258.

[29] M. Halik, H. Klauk, U. Zschieschang, G. Schmid, C Dehm, M. Schütz, S. Maisch, F. Effenberger, M. Brunnbauer, F. Stellacci, Low-voltage organic transistors with an amorphous molecular gate dielectric, *Nature* 2004, **431**, 963– 966.

[30] L.-L. Chua, J. Zaumseil, J.-F. Chang, E. C.-W. Ou, P. K.-H. Ho, H. Sirringhaus and R. H. Friend, General observation of n-type field-effect behaviour in organic semiconductors, *Nature* 2005, **434**, 194–199.

[31] S. Kobayashi, T. Nishikawa, T. Takenobu, S. Mori, T. Shimoda, T. Mitani, H. Shimotani, N. Yoshimoto, S. Ogawa and Y. Iwasa, Control of carrier density by self-assembled monolayers in organic field-effect transistors, *Nat. Mater.* 2004, **3**, 317– 322.

[32] F. Patolsky, G. Zheng and C. M. Lieber, Fabrication of silicon nanowire devices for ultrasensitive, label-free, real-time detection of biological and chemical species, *Nat. Protoc.* 2006, **1**, 1711–1724.

[33] A. Ulman, Formation and structure of self-assembled monolayers, *Chem. Rev.* 1996, **96**, 1533–1554.

[34] R. Tian, O. Seitz, M. Li, W. Hu, Y. J. Chabal, J. Gao, Infrared Characterization of Interfacial Si–O Bond Formation on Silanized Flat SiO2/Si Surfaces *Langmuir* 2010, **26**, 4563–4566.

[35] C. P. Tripp and M. L. Hair, Reaction of chloromethylsilanes with silica: a low-frequency infrared study, *Langmuir* 1991, **7**, 923–927.

[36] N. Sugimoto, A. Narumil, T. Satoh, H. Kaga and T. Kakuchi, A convenient synthesis of functionalized alkoxyamines as initiators for living free radical polymerization, *Polym. Bull.* 2003, **49**, 337–340.

[37] C. J. Hawker, A. W. Bosman and E. Harth, New polymer synthesis by nitroxide mediated living radical polymerizations, *Chem. Rev.* 2001, **101**, 3661–3688.

[38] C. J. Hawker, G. G. Barclay, A. Orellana, J. Dao and W. Devonport, Initiating systems for nitroxide-mediated "living" free radical polymerizations: synthesis and evaluation, *Macromolecules* 1996, **29**, 5245–5254.

[39] Y. Miura, K. Hirota, H. Moto and B. Yamada, High-Yield Synthesis of Functionalized Alkoxyamine Initiators and Approach to Well-Controlled Block Copolymers Using Them, *Macromolecules* 1999, **32**, 8356–8362.

[40] T. J. Connolly, M. V. Baldovi, N. Mohtat and J. C. Scaiano, Photochemical synthesis of TEMPO-capped initiators for "living" free radical polymerization, *Tetrahedron Lett.* 1996, **37**, 4919–4922.

[41] F. Chen, Z. Cai, Y. Huang, W. Luo and J. Chen, Synthesis and characterization of copolymer grafted magnetic nanoparticles via surface-initiated nitroxide-mediated radical polymerization, *Polym. Eng. Sci.* 2013, **53**, 956–962.

[42] J.-M. Moon, B.-S. Kim, H. J. Paik, J.-O. Lee, E. Mouri and K. Yoshinaga, Structural estimation of particle arrays at air–water interface based on silica particles with well-defined and highly grafted poly(methyl methacrylate, *Polym. Eng. Sci.* 2010, **50**, 1067–1074.

[43] M. Salami-Kalajahi, V. Haddadi-Asl, F. Behboodi-Sadabad, S. Rahimi-Razin and H. Roghani-Mamaqani, Properties of PMMA/Carbon nanotubes nanocomposites prepared by "grafting through" method, *Polym. Composite* 2012, **33**, 215–224.

[44] T. A. Pham, J. S. Kim, D. Kim and Y.-T. Jeong, Facile preparation of water-dispersible graphene nanosheets by covalent functionalization with poly(3-aminobenzene sulfonic acid), *Polym. Eng. Sci.* 2012, **52**, 1854–1861.

[45] J. C. Chen, W. Q. Luo, H. D. Wang, J. M. Xiang, H. F. Jin, F. Chen and Z. W. Cai, A versatile method for the preparation of end-functional polymers onto SiO2 nanoparticles by a combination of surface-initiated ATRP and Huisgen [3 + 2] cycloaddition, *Appl. Surf. Sci.* 2010, **256**, 2490–2495.

[46] J. Chen, M. Hu, W. Zhu and Y. Li, Synthesis of well-defined structurally silica–nonlinear polymer core–shell nanoparticles via the surface-initiated atom transfer radical polymerization, *Appl. Surf. Sci.* 2011, **257**, 6654–6660.

[47] J. C. Chen, H. D. Wang, W. Q. Luo, J. M. Xiang, L. H. Zhang and B. B. Sun, Preparation of poly(ε-caprolactone)@attapulgite nanocomposites via a combination of controlled ring-opening polymerization and click chemistry, *Colloid. Polym. Sci.* 2010, **288**, 173–179.

[48] J. T. Yang, M. R. Loos, D. L. Feke and I. Manas-Zloczower, The effect of dispersants on the tensile properties of carbon nanotube/vinyl ester composites, *Polym. Composite* 2012, **33**, 412–419.

[49] J. H. Wang, G. Z. Liang, H. X. Yan and S. B. He, Mechanical and thermal properties of functionalized multiwalled carbon nanotubes/cyanate ester composite, *Polym. Eng. Sci.* 2009, **49**, 680–684.

[50] J. Pyun, S. Jia, T. Kowalewski, G. D. Patterson and K. Matyjaszewski, Synthesis and characterization of organic/inorganic hybrid nanoparticles: kinetics of surface-initiated atom transfer radical polymerization and morphology of hybrid nanoparticle ultrathin films, *Macromolecules* 2003, **36**, 5094–5104.

[51] L. Wang and B, C. Benicewicz, Synthesis and characterization of dye-labeled poly(methacrylic acid) grafted silica nanoparticles, *ACS Macro Lett*. 2013, **2**, 173–176.

[52] L. Wang, M. Cole, J. Li, Y. Zheng, Y. P. Chen, K. P. Miller, A. W. Decho and B. C. Benicewicz, Polymer grafted recyclable magnetic nanoparticles, *Polym. Chem.* 2015, **6**, 248–255.

[53] J. Bonilla-Cruz, T. Lara-Ceniceros, E. Saldivar-Guerra and E. Jimenez-Regalado, Towards Controlled Graft Polymerization of Poly[styrene-co-(maleic anhydride)] on Functionalized Silica Mediated by Oxoaminium Bromide Salt. Facile Synthetic Pathway Using Nitroxide Chemistry, *Macromol. Rapid Commun.* 2007, **28**, 1397–1403.

[54] V. A. Golubev, R. I. Zhdanov, V. M. Gida and E. G. Rozantsev, *Russ. Chem. Bull.* 1971, **20**, 768–770. (English translation)

[55] G. M. Sheldrick, *Acta Cryst.* 2008, **A64**, 112–122.

[56] P. J. Launer, Infrared Absorption Bands Characteristic of the Si–CH2CH2CN and Si–CH2CH2CH2CN Groups, *Appl. Spectrosc.* 1968, **22**, 201–203.

[57] W. Hönle, V. Manríquez and H. G.Von Schnering, Structures of solvated hexaphenyldisiloxanes, *Acta Cryst.* 1990, **c46**, 1982–1984.

[58] A. D. Becke, Density-functional thermochemistry. III. The role of exact exchange, *J. Chem. Phys.*1993, **98**, 5648–5652.

[59] M. J. Frisch, J. A. Pople, J. S. Binkley. Self-consistent molecular orbital methods 25. Supplementary functions for Gaussian basis sets, *J. Chem. Phys.* 1984, **80**, 3265–3269.

[60] M. J. Frisch, G. W. Trucks, H. B. Schlegel, G. E. Scuseria,, M. A. Robb, J. R. Cheeseman, G. Scalmani, V. Barone, B. Mennucci, G. A. Petersson, H. Nakatsuji, M. Caricato, X. Li, H. P. Hratchian, A. F. Izmaylov, J. Bloino, G. Zheng, J. L. Sonnenberg, M. Hada, M. Ehara, K. Toyota, R. Fukuda, J. Hasegawa, M. Ishida, T. Nakajima, Y. Honda, O. Kitao, H. Nakai, T. Vreven, J. A. Montgomery Jr.,, J. E. Peralta, F. Ogliaro, M. Bearpark, J. J. Heyd, E. Brothers, K. N. Kudin, V. N. Staroverov, R. Kobayashi, J. Normand, K. Raghavachari, A. Rendell, J. C. Burant, S. S. Iyengar, J. Tomasi, M. Cossi,, N. Rega, N. J. Millam, M. Klene, J. E. Knox, J. B. Cross, V. Bakken, C. Adamo, J. Jaramillo, R. Gomperts, R. E. Stratmann, O. Yazyev, A. J. Austin, R. Cammi, C. Pomelli, J. W. Ochterski, R. L. Martin, K. Morokuma, V. G. Zakrzewski, G. A. Voth, P. Salvador, J. J. Dannenberg, S. Dapprich, A. D. Daniels,, Ö. Farkas, J. B. Foresman, J. V. Ortiz, J. Cioslowski, and D. J. Fox, D. J. (2009). Gaussian 09 Revision A.1 [computer software].Wallingford, CT, USA: Gaussian.

[61] V. Barone, M. Cossi and J. Tomasi, A new definition of cavities for the computation of solvation free energies by the polarizable continuum model. *J. Chem. Phys.* 1997, **107**, 3210–3212.

[62] U. Losehand, N. W. Mitzel and D. W. H. Rankin, Synthesis and molecular structures of N,N-dimethylhydroxyl-amino-trichlorosilane and –germane, *J. Chem. Soc., Dalton Trans.*1999, 4291-4297.

[63] N. W. Mitzel and U. Losehand, β-donor bonds in compounds containing SiON fragments, *Angew. Chem. Int. Ed. Engl.* 1997, **36**, 2807–2809.

[64] N. W. Mitzel, U. Losehand, β-Donor interactions of exceptional strength in *N,N*-dimethylhydroxylaminochlorosilane, $C_lH_2SiONMe_2$, *J. Am. Chem. Soc.* 1998, **120**, 7320–7327.

[65] N. W. Mitzel, U. Losehand, B. Bauer, SiONB Unit as reference for blocked Si...N interactions in SiON compounds, *Inorg. Chem.* 2000, **39**, 1998–2000.

[66] N. W. Mitzel, U. Losehand, A. Wu, D. Cremer, D. W. H. Rankin, (N,N-Dimethylaminoxy)trifluorosilane: Strong, dipole moment driven dhanges in the molecular geometry studied by experiment and theory in solid, gas, and solution phases, *J. Am. Chem. Soc.* 2000, **122**, 4471–4482.

[67] T. Foerster, D. A. Wann, D. W. H. Rankin, Extremely narrow SiON angles in siloxy-substituted nitrogen-containing rings: a computational investigation. *Dalton Trans.* 2008, 5999–6004.

[68] S. Stefan, F. Belaj, T. Madl, R. Pietschinig, A Radical approach to hydroxylaminotrichlorosilanes: synthesis, reactivity, and crystal structure of TEMPO-SiCl$_3$ (TEMPO= 2,2,6,6-Tetramethylpiperidine-N-oxyl), *Eur. J. Inorg. Chem.*2010, **2**, 289–297.

[69] G. Orcel, J. Phalippou, L. L. Hench, Structural changes of silica xerogels during low temperature dehydration. *J. Non-Crystal. Solids* 1986, **88**, 114–130.

[70] R. Al-Oweini, H. El-Rassy, Synthesis and characterization by FTIR spectroscopy of silica aerogels prepared using several Si(OR)4 and R''Si(OR')3 precursors. *J. Mol. Struct.* 2009, **919**, 140–145.

[71] L. Rintoul, A. S. Micallef, D. A. Reid, S. E. Bottle, The vibrational spectrum of the stable free radical 1,1,3,3-tetramethylisoindolin-2-yloxyl. *Spectrochim. Acta Part A* 2006, **63**, 398–402.

[72] C. J. Brinker, G. W. Scherer, Sol-Gel Science: The physics and chemistry of sol-gel processing, Academic Press, inc. San Diego, CA., 907, 1990.

[73] R. S. A. deLange, J. H. A. Hekkink, K. Keizer and A. J. Burggraaf, Polymeric-silica-based sols for membrane modification applications: sol-gel synthesis and characterization with SAXS, *J. Non-Cryst. Solids* 1995, **191**, 1–16.

[74] R. F. S. Lenza and W. L. Vasconcelos, Preparation of silica by sol-gel method using formamide *Mat. Res.* 2001, **2**, 189–194.

[75] R. Winter, J. B. Chan, R. Frattini and J. Jonas, The effect of fluoride on the sol-gel process, *J. Non-Cryst. Solids* 1988, **105**, 214–222.

[76] Sol-Gel Chemistry. http:// www.psrc.usm.edu/mauritz/solgel.htm. 7/29/1999.

[77] M. Schraml-Marth, K. L Walther, A. Wokaun, B. E. Handy and A. Baiker, Porous silica gels and TiO2/SiO2 mixed oxides prepared via the sol-gel process: characterization by spectroscopic techniques, *J. Non-Cryst. Solids* 1992, **143**, 93–111.

[78] G. Socrates, Infrared and Raman characteristics group frecuencies: Tables and Charts, third ed. Wiley, 201, 45.

[79] S. Stefan, F. Belaj, T. Madl and R. Pietschnig, A radical approach to hydroxylaminotrichlorosilanes: synthesis, reactivity, and crystal structure of

TEMPO-SiCl$_3$ (TEMPO = 2,2,6,6-Tetramethylpiperidine-*N*-oxyl), *Eur. J. Inorg. Chem.* 2010, **2**, 289–297.

[80] R. Tian, O. Seitz, M. Li, W. Hu, Y. J. Chabal and J. Gao, Infrared Characterization of Interfacial Si−O Bond Formation on Silanized Flat SiO2/Si Surfaces, *Langmuir* 2010, **26**, 4563–4566.